

# Highly efficient blue emitting materials based on indenopyrazine derivatives for OLEDs [Invited]

Hayoon Lee,<sup>1</sup> Young IL Park,<sup>2</sup> Beomjin Kim,<sup>1</sup> Ji-Hoon Lee,<sup>3</sup> and Jongwook Park,<sup>1,\*</sup>

<sup>1</sup>Department of Chemistry, Catholic University of Korea, Bucheon, 420-743, South Korea

<sup>2</sup>Research Center for Green Fine Chemicals, Korea Research Institute of Chemical Technology, Ulsan, 681-802, South Korea

<sup>3</sup>Department of Polymer Science and Engineering, Korea National University of Transportation, Chungju, 380-702, South Korea

\*hahapark@catholic.ac.kr

**Abstract:** Two indenopyrazine compounds for organic light emitting diodes were synthesized with phenanthrene or pyrene side groups that have high photoluminescence (PL) quantum efficiency (QE); 6,6,12,12-Tetraethyl-2,8-di-phenanthren-9-yl-6,12-dihydro-diindeno[1,2-b;1',2'-e]pyrazine (PA-EIP) and 2-(10b,10c-Dihydro-pyren-1-yl)-6,6,12,12-tetraethyl-8-pyren-1-yl-6,12-dihydro-diindeno[1,2-b;1',2'-e]pyrazine (PY-EIP). The PL spectra of PA-EIP and PY-EIP in film state were 440 nm and 468nm in the blue region, respectively. T<sub>d</sub> values for PA-EIP and PY-EIP were very high at 432°C and 441°C. T<sub>m</sub> values were 385°C and 390°C for PA-EIP and PY-EIP. When the synthesized compounds were used as emitting layers in non-doped OLED devices, PA-EIP and PY-EIP showed luminance efficiencies of 1.35 and 5.15 cd/A, power efficiencies of 0.69 and 2.81 lm/W, and CIEs of (0.17, 0.15) and (0.19, 0.30), respectively. This result shows that efficiency of final emitter increases with increasing efficiency of side group. Additionally, in the solution-processed white OLED devices using PY-EIP as one of emitting materials, the device showed high luminance efficiency of 3.95 cd/A, power efficiency of 2.45 lm/W and CIE value of (0.269, 0.294) at 6 V.

©2014 Optical Society of America

**OCIS codes:** (160.2540) Fluorescent and luminescent materials; (250.5230) Photoluminescence; (300.6280) Spectroscopy, fluorescence and luminescence; (230.3670) Light-emitting diodes.

---

## References and Links

1. C. W. Tang and S. A. Van Slyke, "Organic electroluminescent diodes," *Appl. Phys. Lett.* **51**(12), 913–915 (1987).
2. M. F. Wu, S. J. Yeh, C. T. Chen, H. Murayama, T. Tsuboi, W. S. Li, I. Chao, S. W. Liu, and J. K. Wang, "The Quest for High-Performance Host Materials for Electrophosphorescent Blue Dopants," *Adv. Funct. Mater.* **17**(12), 1887–1895 (2007).
3. Y. Dienes, S. Durben, T. Kárpáti, T. Neumann, U. Englert, L. Nyulászi, and T. Baumgartner, "Selective tuning of the band gap of  $\pi$ -conjugated dithieno[3,2-b:2',3'-d]phospholes toward different emission colors," *Chemistry* **13**(26), 7487–7500 (2007).
4. C. Pérez-Bolivar, S. Y. Takizawa, G. Nishimura, V. A. Montes, and P. Anzenbacher, Jr., "High-efficiency tris(8-hydroxyquinoline)aluminum (Alq3) complexes for organic white-light-emitting diodes and solid-state lighting," *Chemistry* **17**(33), 9076–9082 (2011).
5. M. C. Gather, A. Kohnen, A. Falcou, H. Becker, and K. Meerholz, "Solution-processed full-color polymer organic light-emitting diode displays fabricated by direct photolithography," *Adv. Funct. Mater.* **17**(2), 191–200 (2007).
6. C. Liu, Y. Li, Y. Zhang, C. Yang, H. Wu, J. Qin, and Y. Cao, "Solution-processed, undoped, deep-blue organic light-emitting diodes based on starburst oligofluorenes with a planar triphenylamine core," *Chemistry* **18**(22), 6928–6934 (2012).
7. S. K. Kim, Y. I. Park, I. N. Kang, J. H. Lee, and J. W. Park, "New deep-blue emitting materials based on fully substituted ethylene derivatives," *J. Mater. Chem.* **17**(44), 4670–4678 (2007).
8. S. K. Kim, B. Yang, Y. Ma, J. H. Lee, and J. Park, "Exceedingly efficient deep-blue electroluminescence from new anthracenes obtained using rational molecular design," *J. Mater. Chem.* **18**(28), 3376–3384 (2008).

9. B. Kim, Y. Park, J. Lee, D. Yokoyama, J. H. Lee, J. Kido, and J. Park, "Synthesis and electroluminescence properties of highly efficient blue fluorescence emitters using dual core chromophores," *J. Mater. Chem. C* **1**(3), 432–440 (2012).
10. H. Park, J. Lee, I. Kang, H. Y. Chu, J. I. Lee, S. K. Kwon, and Y. H. Kim, "Highly rigid and twisted anthracene derivatives: a strategy for deep blue OLED materials with theoretical limit efficiency," *J. Mater. Chem.* **22**(6), 2695–2700 (2012).
11. Z. Q. Wang, C. Xu, W. Z. Wang, L. M. Duan, Z. Li, B. T. Zhao, and B. M. Ji, "High-color-purity and high-efficiency non-doped deep-blue electroluminescent devices based on novel anthracene derivatives," *New J. Chem.* **36**(3), 662–667 (2012).
12. C. H. Wu, C. H. Chien, F. M. Hsu, P. I. Shih, and C. F. Shu, "Efficient non-doped blue-light-emitting diodes incorporating an anthracene derivative end-capped with fluorene groups," *J. Mater. Chem.* **19**(10), 1464–1470 (2009).
13. S. L. Lai, Q. X. Tong, M. Y. Chan, T. W. Ng, M. F. Lo, S. T. Lee, and C. S. Lee, "Distinct electroluminescent properties of triphenylamine derivatives in blue organic light-emitting devices," *J. Mater. Chem.* **21**(4), 1206–1211 (2011).
14. C. Hosokawa, H. Higashi, H. Nakamura, and T. Kusumoto, "Highly efficient blue electroluminescence from a distyrylarylene emitting layer with a new dopant," *Appl. Phys. Lett.* **67**(26), 3853–3855 (1995).
15. Y. I. Park, J. H. Son, J. S. Kang, S. K. Kim, J. H. Lee, J. W. Park, "Synthesis and electroluminescence properties of novel deep blue emitting 6,12-dihydro-diindeno[1,2-b;1'2'-e]pyrazine derivatives," *Chem. Comm.* **18**, 2143–2145 (2008).
16. X. Kong, A. P. Kulkarni, and S. A. Jenekhe, "Phenothiazine-based conjugated polymers: synthesis, electrochemistry, and light-emitting properties," *Macromolecules* **36**(24), 8992–8999 (2003).
17. D. Wang, Z. Wu, X. Zhang, B. Jiao, S. Liang, D. Wang, R. He, and X. Hou, "Solution-processed organic films of multiple small-molecules and white light-emitting diodes," *Org. Electron.* **11**(4), 641–648 (2010).
18. S. K. Kim, B. Yang, Y. I. Park, Y. Ma, J. Y. Lee, H. J. Kim, and J. Park, "Synthesis and electroluminescent properties of highly efficient anthracene derivatives with bulky side groups," *Org. Electron.* **10**(5), 822–833 (2009).
19. S. L. Murov, I. Carmichael, and G. L. Hug, in *Handbook of Photochemistry 2nd ed*, M. Dekker, ed. (Talyor& Francis, New York, 1993)
20. B. I. Berlman, in *Handbook of Fluorescence Spectra of Aromatic Molecules* (Academic Press, 1971)
21. S. Ates and A. Yildiz, "Determination of the absolute quantum efficiency of the luminescence of crystalline anthracene and of meso-dimeso derivatives using photoacoustic spectroscopy," *J. Chem. Soc., Faraday Trans. 1* **79**(12), 2853–2861 (1983).
22. R. Kato, K. Suzuki, A. Furube, M. Kotani, and K. Tokumaru, "Fluorescence quantum yield of aromatic hydrocarbon crystals," *J. Phys. Chem. C* **113**(7), 2961–2965 (2009).

## 1. Introduction

Since the study of organic light-emitting diodes (OLEDs) began [1], OLEDs have received much attention because of their potential applications in full-color flat panel displays and next generation lighting [2–7]. To date, numerous conjugated organic molecules have been synthesized and reported to exhibit electroluminescence (EL) ranging from red to green and blue. In order to fabricate full color OLED displays, we need high performance red, green and blue-light emitters with high EL efficiencies, good thermal properties, and long device lifetimes as well as pure color coordinates (1931 Commission Internationale de l'Eclairage x,y coordinates (CIE (x,y))). It is extremely difficult to produce highly efficient blue-light emitters with a long device lifetime because of their wide band gap, as wide band gap of blue emitting material makes recombination zone of electrons and holes mismatched. It leads to low EL efficiency as well as short lifetime of OLED device.

Up to date, many types of blue-light emitters including anthracene [8–11], fluorine [12], pyrene [9, 13] and di(styryl)arylene [14] based derivatives have been intensively investigated and attempts have been made to improve their EL properties. In recent, we described initial efforts to harness the properties of indenopyrazine, an imine-substituted heteroaromatic core, for use as a blue emitting material. Indenopyrazine showed several excellent properties: a Commission Internationale de l'Eclairage (CIE) of (0.154, 0.078), an emission band with a full width at half maximum (FWHM) of 47 nm, and very close to the standard used by the National Television System Committee (NTSC) in a non-doped OLED device. However, other emission efficiency properties such as luminance efficiency and power efficiency performance were 2.01 cd/A and 0.92 lm/W, respectively. It shows still lower emission efficiency than other blue emitting materials [15]. In our previous work, there are close correlations between the side-group PL/QE and the PL/QE of the final compound, i.e., when the molecular core structure is the same, the order of the PL efficiencies of the side groups is

consistent with the order of the PL efficiencies of the whole molecules. Also, the introduction of a bulky side group should help to prevent  $\pi$ - $\pi$  stacking interactions, which should lead to limit emission quenching [8].

Recently, solution process of OLED device was an attractive approach because of low cost general lighting applications or display on large area [5,6,16,17]. Although polymer based light-emitting diodes (PLED) should be approached for solution process of OLED, they are generally difficult to purify for PLED devices. Therefore, small molecules for solution processing should have a good solubility and high emission efficiency property.

Based on these results, we designed new blue emitting materials based on indenopyrazine core. Firstly, we placed phenanthrene and pyrene moiety with high PL quantum efficiency in the side of the molecular structure. Secondly, highly twisted side group with core leads to prevent  $\pi$ - $\pi^*$  stacking interactions for high luminance efficiency. Lastly, alkyl group and highly twisted side group make to be good solubility for solution process. The synthesized blue emitting materials are 6,6,12,12-Tetraethyl-2,8-di-phenanthren-9-yl-6,12-dihydro-diindeno[1,2-b;1',2'-e]pyrazine (PA-EIP), 2-(10b,10c-Dihydro-pyren-1-yl)-6,6,12,12-tetraethyl-8-pyren-1-yl-6,12-dihydro-diindeno[1,2-b;1',2'-e]pyrazine (PY-EIP) (see Fig. 1). The thermal and electronic properties of synthesized materials were characterized with differential scanning calorimetry (DSC), thermogravimetric analysis (TGA), cyclic voltammetry (CV), and UV-visible and PL spectroscopy. Multilayered EL devices were fabricated using synthesized materials as non-doped emitting layers and dopant for solution processed white OLED.

## 2. Experimental section

**General method:**  $^1\text{H-NMR}$  spectra were recorded using Bruker Avance 300 instruments and fast atom bombardment (FAB) mass spectra were recorded using a JEOL, JMS-AX505WA, HP5890 series II. The optical absorption spectra were obtained using an HP 8453 UV-VIS-NIR spectrometer. A Perkin-Elmer luminescence spectrometer LS50 (Xenon flash tube) was used for PL and EL spectroscopy. The melting temperatures ( $T_m$ ), glass-transition temperatures ( $T_g$ ), crystallization temperatures ( $T_c$ ), and degradation temperatures ( $T_d$ ) of the compounds were measured by DSC under a nitrogen atmosphere using a DSC2910 (TA Instruments), and TGA was performed using an SDP-TGA2960 (TA Instruments). The redox potentials of the compounds were determined by CV using an AUTOLAB/PG-STAT128N model system with a scan rate of 100 mV/s. The working electrode was formed by depositing a coating of the synthesized materials onto ITO substrates, saturated Ag/AgNO<sub>3</sub> was used as the reference electrode, and acetonitrile (AN) with 0.1 M tetrabutylammonium perchlorate (TBAP) was used as the electrolyte. Ferrocene was used to calibrate the potential as well as for the reversibility criteria. Non-doped blue emitting OLED devices were fabricated with the following structure: ITO/2-TNATA (60 nm)/NPB (15 nm)/DPVBi or synthesized material (30 nm)/Alq<sub>3</sub> or TPBi (30 nm)/LiF (1 nm)/Al (200 nm), where 4,4',4''-tris(N-(2-naphthyl)-N-phenylamino)triphenylamine (2-TNATA) formed the HIL, N,N'-bis(naphthalen-1-yl)-N,N'-bis(phenyl)benzidine (NPB) formed the HTL, 4,4'-bis(2,2-diphenylvinyl)-1,1'-biphenyl (DPVBi) and the synthesized materials formed the EML, Tris(8-hydroxyquinolinato)aluminium (Alq<sub>3</sub>) or (2,2',2''-1,3,5-Benzinetriyl)-tris(1-phenyl-1-H-benzimidazole (TPBi) formed the ETL, lithium fluoride (LiF) formed the EIL, ITO formed the anode, and Al formed the cathode. The organic layer was vacuum-deposited by thermal evaporation at a vacuum base pressure of  $10^{-6}$  Torr and a rate of deposition of 1 Å/s to give an emitting area of 4 mm<sup>2</sup>; the Al layer was continuously deposited under the same vacuum conditions. Solution processing white OLED devices were fabricated with the following structure: ITO/PEDOT:PSS (40 nm)/ 57.5% NPB + 38.3% DPVBi + 4% PY-EIP + 0.2% Rubrene (50 nm)/TPBi (30 nm)/LiF (1 nm)/Al (200 nm). DPVBi, NPB were used for the host substances used in the emitting layer, and PY-EIP and (5,6,11,12)-Tetraphenylnaphthacene (Rubrene) were respectively used as blue and yellow dopant substances. DPVBi: NPB was mixed in a mass ratio of 60:40 for host substances, and DPAVBi with ratio of 4% and Rubrene with ratio of 0.2% were mixed for dopant substances based on the mass of co-host.

Chlorobenzene was used as solvent. A water-dispersed PEDOT/PSS mixture (Baytron P VP CH8000, H. C. Starck GmbH) was spin-coated on top of ITO in air to achieve films (40 nm). The spin-coated films were baked on a hot plate at 110 °C for 5 minutes in air and 200 °C for 5 minutes in a N<sub>2</sub> glove box. The emitting layer was made by spin-coating to obtain a thickness of 50 nm. The solution-processed films were baked on a hot plate (80 °C, 30 min) in a N<sub>2</sub> glove box. Electron-transporting layers, TPBi with a thickness of 20 nm were deposited by vacuum evaporation (at a pressure about 10<sup>-6</sup> Torr). LiF (1 nm) and Al films were sequentially deposited on the electron-transporting layer under vacuum (at a pressure about 10<sup>-6</sup> Torr). The current–voltage (I–V) characteristics of the fabricated OLED devices were obtained using a Keithley 2400 Source Meter. Light intensity was measured using a Minolta CS-1000A spectroradiometer.

**General syntheses of new materials:** Indenopyrazine core was synthesized according to the reference procedures [15]. The materials were synthesized by a Suzuki aryl-aryl coupling reaction in the presence of a Pd catalyst. A typical synthetic procedure was as follows: To 2,8-dibromo-6,6,12,12-tetraethyl-6,12-dihydrodiindeno[1,2-b:1,2-e]pyrazine (1 g, 1.90 mmol) and Phenanthrene-9-yl-boronic acid (1.2 g, 5.7 mmol) in a 250 mL round-bottomed flask under a nitrogen atmosphere were added Pd(OAc)<sub>2</sub> (0.01 g, 0.05 mmol), tri-cyclohexylphosphine (0.03 g, 0.11 mmol), 100 ml of THF anhydrous, and 10% tetrabutylammonium hydroxide 7 ml. The temperature was increased to reflux temperature, and the reaction was monitored by TLC. When the reaction was complete, the product was extracted with water and toluene. The organic extract was dried over MgSO<sub>4</sub>, filtered, and the solvent was removed in vacuo. The resulting crude mixture was passed through a short column of silica using THF as the eluent, and the product was recrystallized from THF to obtain a yellow solid.

*Synthesis of 6,6,12,12-Tetraethyl-2,8-di-phenanthren-9-yl-6,12-dihydro-diindeno[1,2-b;1',2'-e]pyrazine (PA-EIP)*

The yield was 73%. <sup>1</sup>H NMR(300MHz, CDCl<sub>3</sub>): δ(ppm) 0.51-0.56(m, *J* = 7.3 Hz, 12H), 2.09-2.21(m, *J* = 7.3 Hz, 4H), 2.37-2.49(m, *J* = 7.1 Hz, 4H), 7.54-7.59(t, *J* = 8.0 Hz, 2H), 7.63-7.73(m, *J* = 7.2 Hz, 10H), 7.80(s, 2H), 7.95-7.99(t, *J* = 7.7 Hz, 4H), 8.25-8.27(d, *J* = 8.3 Hz, 2H), 8.74-8.77(d, *J* = 8.0 Hz, 2H), 8.80-8.83(d, *J* = 8.3 Hz, 2H), <sup>13</sup>C NMR(300MHz, CDCl<sub>3</sub>): 9.0, 31.4, 54.3, 121.2, 122.8, 123.2, 125.1, 126.7, 126.8, 126.9, 127.0, 127.1, 127.7, 128.9, 129.6, 130.3, 131.0, 131.4, 131.8, 138.7, 139.2, 142.0, 150.0, 152.4, 163.3, FT-IR (KBr cm<sup>-1</sup>): 3070, 2959, 2918, 1610, 1449, 1367, 1280, 1225, 1177, 1116, 1038, 887, 835, 743, 721, 659, 488, 422, Fab<sup>+</sup>-Mass m/e: 720

*Synthesis of 2-(10b,10c-Dihydro-pyren-1-yl)-6,6,12,12-tetraethyl-8-pyren-1-yl-6,12-dihydro-diindeno[1,2-b;1',2'-e]pyrazine (PY-EIP)*

The yield was 83%. <sup>1</sup>H NMR(300MHz, CDCl<sub>3</sub>): δ(ppm) 0.55-0.60(m, *J* = 7.1 Hz, 12H), 2.13-2.25(m, *J* = 7.4 Hz, 4H), 2.41-2.52(m, *J* = 6.8 Hz, 4H), 7.74-7.77(d, *J* = 7.8 Hz, 4H), 8.04-8.14(m, *J* = 5.1 Hz, 10H), 8.18-8.30(m, *J* = 8.3 Hz, 10H), <sup>13</sup>C NMR(300MHz, CDCl<sub>3</sub>): 9.1, 31.4, 54.3, 121.2, 124.9, 125.1, 125.2, 125.3, 125.4, 125.7, 126.3, 127.6, 127.7, 127.8, 127.9, 128.8, 130.2, 131.0, 131.2, 131.7, 138.2, 138.6, 142.4, 150.1, 152.4, 163.4, FT-IR (KBr cm<sup>-1</sup>): 3036, 2960, 1602, 1450, 1365, 1286, 1227, 1174, 1118, 840, 756, 712, 680, 625, 479, Fab<sup>+</sup>-Mass m/e: 769

### 3. Result and discussion

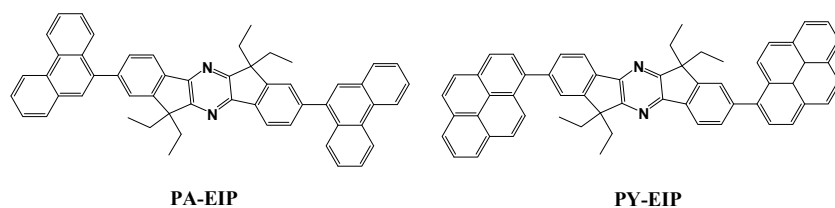


Fig. 1. Chemical structure of new indenopyrazine blue emitting materials.

Figure 1 shows the chemical structures of the synthesized material. The synthesis routes are shown in Fig. 2. Synthesized materials were synthesized according to literature procedures [15]. These final compounds were purified with column chromatography using silica gel and recrystallization, producing very pure powder that we characterized with NMR, FT-IR, and FAB-MS analysis.

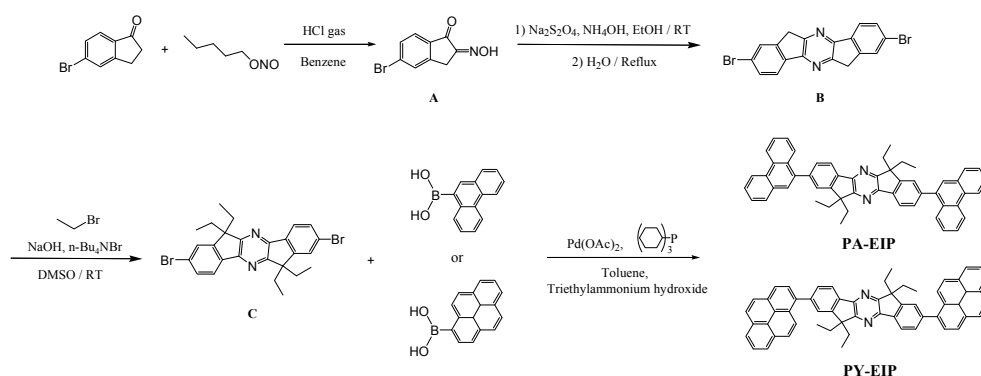


Fig. 2. Synthetic route of new indenopyrazine blue emitting materials.

The thermal stabilities of the synthesized materials were measured by thermal gravimetric analysis (TGA) and differential scanning calorimetry (DSC), as summarized in Table 1. The  $T_d$  values for PA-EIP and PY-EIP were high: 432 °C and 441 °C, respectively. The values for  $T_m$  were 385 °C and 390 °C, for PA-EIP and PY-EIP, respectively.  $T_d$  and  $T_m$  of synthesized materials exhibit better thermal stability compared to DPVBi (204 °C), a commercial blue emitting material used in blue OLEDs. We believe that the thermal properties of the films used in OLEDs are strongly associated with device lifetimes because of Joule heating during device operation.

**Table 1. Thermal properties of the synthesized materials.**

| Compounds | $T_m$ /°C | $T_d$ /°C |
|-----------|-----------|-----------|
| PA-EIP    | 385       | 432       |
| PY-EIP    | 390       | 441       |

$T_m$ : melting temperature,  $T_d$ : decomposition temperature (5% weight loss)

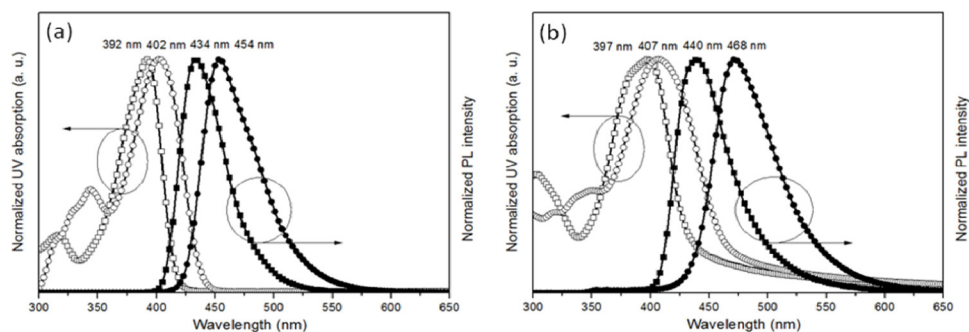


Fig. 3. UV-Visible absorption and PL spectra in (a) solution and (b) film state; PA-EIP (square), PY-EIP (circle).

**Table 2. Optical properties of the synthesized materials.**

| Compounds | Solution <sup>a</sup>     |                           | Film on glass             |                           | HO<br>MO<br>(eV) | LU<br>MO<br>(eV) | Band<br>gap |
|-----------|---------------------------|---------------------------|---------------------------|---------------------------|------------------|------------------|-------------|
|           | UV <sub>max</sub><br>(nm) | PL <sub>max</sub><br>(nm) | UV <sub>max</sub><br>(nm) | PL <sub>max</sub><br>(nm) |                  |                  |             |
| PA-EIP    | 392                       | 434                       | 397                       | 440                       | 6.08             | 3.15             | 2.93        |
| PY-EIP    | 402                       | 454                       | 407                       | 468                       | 5.68             | 2.92             | 2.76        |

a: THF solution ( $1 \times 10^{-5}$  M)

UV-visible absorption (UV-visible) and PL spectra in THF solution state and the thin-film state were measured as shown in Table 2 and Fig. 3. In THF solution state, the UV-visible maxima were 392 nm and 402 nm and PL spectral maxima were 434 nm and 454 nm for PA-EIP and PY-EIP in the blue region, respectively. The PL spectrum maximum of PY-EIP was red-shifted by 20 nm relative to maximum of PA-EIP. It means that pyrene group was more conjugated than phenanthrene group of PA-EIP in the indenopyrazine core. In the thin-film state, the UV-visible maximum value of PA-EIP and PY-EIP shows 397 nm and 407 nm, respectively, which are similar to that of solution state. However, the PL spectra of PA-EIP and PY-EIP in film state were found to be 6 nm and 14 nm red-shifted with respect to those of their solutions. It means that pyrene group of PY-EIP was more intermolecular packing than phenanthrene group of PA-EIP [8,18].

In order to measure the HOMO values of the synthesized materials, cyclic voltammetry (CV) analyses were carried out. The HOMO, LUMO levels and energy band gaps of synthesized materials were estimated by CV and the analysis of absorption edge with a plot of  $(h\nu)$  vs.  $(ah\nu)^2$  where  $a$ ,  $h$ , and  $\nu$  are absorbance, Planck's constant, and the frequency of light, as summarized in Table 2. As shown in Table 2, the HOMO levels were 6.08 eV and 5.68 eV and LUMO levels were 3.15 eV and 2.92 eV for PA-EIP and PY-EIP in the blue region, respectively. The band gaps of PA-EIP and PY-EIP were 2.93 eV and 2.76 eV. This result agreed with the red-shifted PL spectrum of PY-EIP compared to that of PA-EIP in that pyrene group in PY-EIP increased conjugation in the core group, which stabilizes and reduces the band gap.

Non-doped OLED devices were fabricated using the synthesized materials as the emitting layer in the following structure: ITO/2-TNATA (60nm)/NPB (15 nm)/synthesized material (30 nm)/Alq<sub>3</sub> (30 nm)/LiF (1 nm)/Al, where 2-TNATA was used for the hole injection layer (HIL), NPB for the hole transport layer (HTL), and Alq<sub>3</sub> for the electron transport layer (ETL).

**Table 3. EL performances of synthesized material: ITO/2-TNATA (60 nm)/NPB (15 nm)/synthesized material (30 nm)/Alq<sub>3</sub> (30 nm)/LiF (1 nm)/Al (200 nm) at 10 mA/cm<sup>2</sup>**

| Compounds           | Voltage (V) | Luminance efficiency (cd/A) | Power Efficiency (lm/W) | Side group QE <sup>b</sup> | CIE (x, y)   |
|---------------------|-------------|-----------------------------|-------------------------|----------------------------|--------------|
| PA-EIP              | 6.8         | 1.35                        | 0.69                    | 0.14                       | (0.17, 0.15) |
| PY-EIP              | 6.3         | 5.15                        | 2.81                    | 0.69                       | (0.19, 0.30) |
| TP-EPY <sup>a</sup> | 7.5         | 2.01                        | 0.92                    | 0.29                       | (0.15, 0.08) |
| PA-EPY <sup>a</sup> | 7.8         | 4.11                        | 1.66                    | 0.41                       | (0.19, 0.25) |

a) Reference [15], b) Quantum efficiency

The EL performances of the devices for a current density of 10 mA/cm<sup>2</sup> are summarized in Table 3. The luminance efficiencies were 1.35 and 5.15 cd/A, power efficiencies were 0.69 and 2.81 lm/W, and CIEs were (0.17, 0.15) and (0.19, 0.30), for PA-EIP and PY-EIP, respectively. When device efficiencies of PA-EIP and PY-EIP are compared with those of our previous result using indenopyrazine core, efficiencies of the final emitters are correlated with efficiencies of side group. That is, PL efficiency of side groups increases in the order of phenanthrene (0.14) [19] < *ter*-phenyl (0.29) [8,20] < phenyl anthracene (0.41) [21] < pyrene (0.69) [22], and the device efficiencies of the final emitters also increase in the order of PA-EIP (1.35 cd/A) < TP-EPY (2.01 cd/A) < PA-EPY (4.11 cd/A) < PY-EIP (5.15 cd/A). In other words, efficiency of final emitter was found to increase with increasing efficiency of side group. These results are identical to those of our previous study using anthracene cored emitters, and clearly show that the side group efficiency is an important key in maximizing EL efficiency of the final emitters [8].

When EL spectra and PL spectra in film state overlapped, EL spectrum was broader than PL spectrum around 550 nm (see Fig. 4). EL spectrum was thought to be caused by the emitting material and Alq<sub>3</sub> interface.

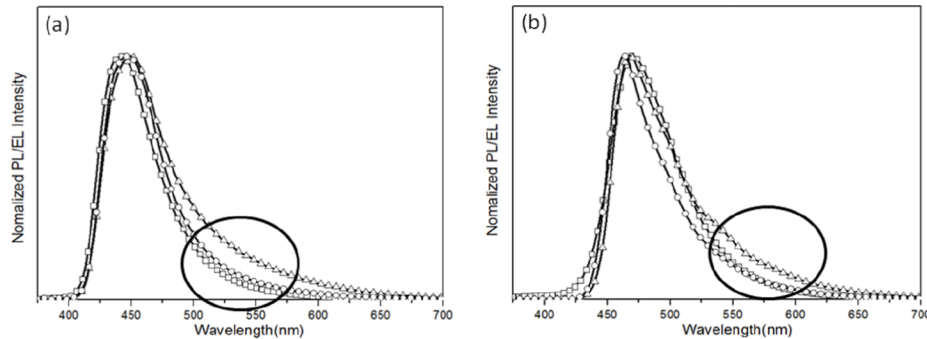


Fig. 4. PL spectrum of film state and EL spectra of non-doping OLED device: ITO/2-TNATA (60 nm)/NPB (15 nm)/(a) PA-EIP or (b) PY-EIP (30 nm)/Alq<sub>3</sub> or TPBi (30 nm)/LiF (1 nm)/Al (200 nm): PL spectrum of film state (square), TPBi (circle), Alq<sub>3</sub> (triangle).

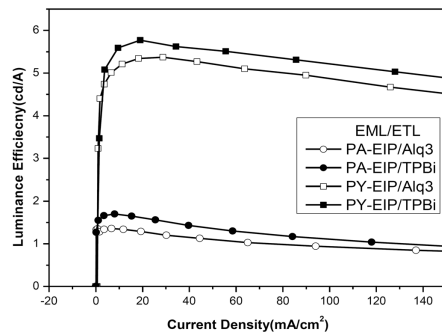


Fig. 5. Luminance Efficiency of non-doped OLED device: ITO/2-TNATA (60 nm)/NPB (15 nm)/PA-EIP or PY-EIP (30 nm)/Alq<sub>3</sub> or TPBi (30 nm)/LiF (1 nm)/Al (200 nm): (○) PA-EIP/Alq<sub>3</sub>, (●) PA-EIP/TPBi, (□) PY-EIP/Alq<sub>3</sub>, (■) PY-EIP/TPBi.

**Table 4. EL performances of synthesized material: ITO/2-TNATA (60 nm)/NPB (15 nm)/synthesized material (30 nm)/Alq<sub>3</sub> or TPBi (30 nm)/LiF (1 nm)/Al (200 nm) at 10 mA/cm<sup>2</sup>**

| Compounds | ETL              | Voltage (V) | Brightness (cd/m <sup>2</sup> ) | Luminance efficiency (cd/A) | Power Efficiency (lm/W) | FWHM | CIE (x, y)   |
|-----------|------------------|-------------|---------------------------------|-----------------------------|-------------------------|------|--------------|
| PA-EIP    | Alq <sub>3</sub> | 6.8         | 136                             | 1.35                        | 0.69                    | 61   | (0.17, 0.15) |
|           | TPBi             | 6.1         | 171                             | 1.69                        | 0.96                    | 54   | (0.16, 0.10) |
| PY-EIP    | Alq <sub>3</sub> | 6.3         | 535                             | 5.15                        | 2.81                    | 57   | (0.19, 0.30) |
|           | TPBi             | 5.0         | 573                             | 5.61                        | 3.86                    | 52   | (0.16, 0.23) |

To test this hypothesis, TPBi has a lower HOMO level than Alq<sub>3</sub>, which improves hole blocking. Figure 4 shows that EL spectra of synthesized material were reduced broaden EL spectrum about 550 nm. Therefore, when TPBi was used as ETL material, PA-EIP and PY-EIP respectively showed luminance efficiencies of 1.69 cd/A, 5.61 cd/A and power efficiencies of 0.96 lm/W, 3.86 lm/W (see Fig. 5). Power efficiencies were respectively improved by 39% and 37% and CIE value was blue shifted according to the hole blocking effect of TPBi, when compared to the device that uses Alq<sub>3</sub> as ETL material. (see Table 4).

Solution processed white OLEDs (WOLEDs) are receiving the spotlight in the fields of OLED backlight and light. In addition, PY-EIP has good solubility in organic solvent because it has an alkyl group and highly twisted molecular structure. Therefore we fabricated solution-processed white OLED devices using PY-EIP as the emitting material in the following structure: ITO/PEDOT:PSS (40 nm)/ 57.5% NPB + 38.3% DPVBi + 4% PY-EIP + 0.2% Rubrene (50 nm)/TPBi (30 nm)/LiF (1 nm)/Al (200 nm). PEDOT:PSS and the emitting layer were made by using a spin-coating method, and ETL layer and LiF/Al electrode were fabricated through a vapor deposition method. NPB and DPVBi were used as co-host materials which have HTL property and wide band gap like a blue emitter [17]. PY-EIP and Rubrene were each used as blue dopant and yellow dopant.

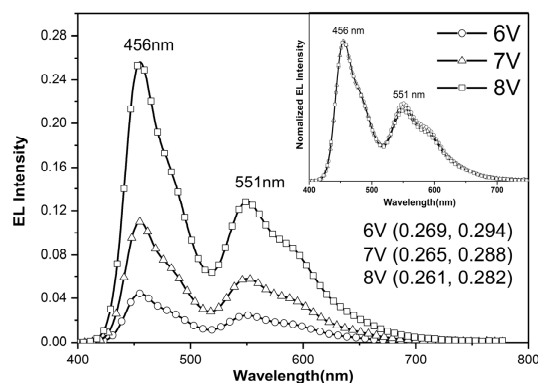


Fig. 6. White EL spectra of solution process OLED device: ITO/PEDOT(40 nm)/NPB(57.5%) + DPVBi (38.3%) + PY-EIP(4%) + Rubrene(0.2%) (50 nm)/TPBi (30 nm)/LiF (1 nm)/Al (200 nm): (○) 6V, (△) 7V, (□) 8V.

**Table 5. EL performances of synthesized material: ITO/PEDOT(40 nm)/NPB(57.5%) + DPVBi (38.3%) + PY-EIP(4%) + Rubrene(0.2%) (50 nm)/TPBi (30 nm)/LiF (1 nm)/Al (200 nm)**

| Current Density (mA/cm <sup>2</sup> ) | Voltage (V) | Brightness (cd/m <sup>2</sup> ) | Luminance Efficiency (cd/A) | Power Efficiency (lm/W) | EL maximum Peak (nm) | CIE (x, y)  |
|---------------------------------------|-------------|---------------------------------|-----------------------------|-------------------------|----------------------|---|
| 20                                    | 5.6         | 830                             | 3.95                        | 2.45                    | 456, 551             | 6 V (0.269,0.294)<br>7 V (0.265,0.288)<br>8 V (0.261,0.282) |
| 100                                   | 7.2         | 3944                            | 3.95                        | 1.88                    | 456, 551             |   |

The EL performance of the solution processed white OLED was summarized Fig. 6 and Table 5. The EL spectral maxima of the white OLED device were 456 nm and 551 nm. Luminance efficiency was 3.95 cd/A and power efficiency was 2.45 lm/W. Especially, as shown in Fig. 6, the EL spectra maxima and the CIE value were 456, 551 nm and (0.269, 0.294) at 6 V. The EL spectrum and CIE value were almost independent of the driving voltage (see inserted Fig. 6). These small CIE value shifts offer convenience for commercial display applications.

#### 4. Conclusion

Two new indenopyrazine derivatives, PA-EIP and PY-EIP, were synthesized and electrical properties were characterized.

$T_d$  values for PA-EIP and PY-EIP were very high at 432°C and 441°C.  $T_m$  values were 385°C and 390°C for PA-EIP and PY-EIP.  $T_d$  and  $T_m$  of synthesized materials exhibit superior thermal stability compared to DPVBi, a commercial blue emitting material used in blue OLEDs.

The efficiency of indenopyrazine derivatives can be improved by substituting its high photoluminescent efficiency side group on the core indenopyrazine. The luminance efficiencies were 1.35 and 5.15 cd/A, power efficiencies were 0.69 and 2.81 lm/W, and CIEs were (0.17, 0.15) and (0.19, 0.30), for PA-EIP and PY-EIP, respectively. This result shows that efficiency of final emitter increases with increasing efficiency of side group. It clearly shows that the side group efficiency is an important key in maximizing EL efficiency of the final emitters.

In addition, PY-EIP has good solubility in common organic solvent because it has an alkyl group and highly twisted molecular structure. In the solution-processed white OLED devices using PY-EIP as one of emitting materials, the device showed high luminance efficiency of 3.95 cd/A and power efficiency of 2.45 lm/W. Especially, the EL spectra maxima and the CIE

value were 456, 551 nm and (0.269, 0.294) at 6 V and were almost independent of the driving voltage.

#### **Acknowledgment**

This work was supported by the National Research Foundation of Korea (NRF) grant funded by the Korean government (MEST) (No. 2012001846).